Enhanced tunability and temperature-dependent dielectric characteristics at microwaves of K0.5Na0.5NbO3 thin films epitaxially grown on (100)MgO substrates

Barthélemy Aspe, Xavier Castel, Valérie Demange, Damien Passerieux, Marie-Amandine Pinault-Thaury, François Jomard, Stéphanie Députier, Dominique Cros, Valérie Madrangeas, Valérie Bouquet, et al.

Enhanced tunability and temperature-dependent dielectric characteristics at microwaves of $K_{0.5}Na_{0.5}NbO_3$ thin films epitaxially grown on (100)MgO substrates

B. Aspe[a,b,*], X. Castel[b,*], V. Demange[a], D. Passerieux[c], M.A. Pinault-Thaury[d], F. Jomard[d], S. Députier[a], D. Cros[c], V. Madrangeas[c], V. Bouquet[a], R. Sauleau[b], M. Guilloux-Viry[a,*]

[a]Univ Rennes, CNRS, ISCR UMR 6226, ScanMAT UMS 2001, F-35000, Rennes, France

[b]Univ Rennes, CNRS, IETR UMR 6164, F-35000, Rennes, France

[c]XLIM UMR CNRS 7252, Faculté des Sciences et Techniques, Université de Limoges, 123 avenue Albert Thomas, F-87060 Limoges France

[d]Université Paris-Saclay, UVSQ, CNRS, GEMaC, F-78000 Versailles, France

Corresponding authors:

Barthélemy Aspe: email adress: barthelemy.aspe@list.lu

ORCID identifier: 0000-0001-8927-4013

Xavier Castel email adress: xavier.castel@univ-rennes1.fr

ORCID identifier: 0000-0001-6661-728X

Maryline Guilloux-Viry: email adress: maryline.guilloux-viry@univ-rennes1.fr

ORCID identifier: 0000-0001-7773-1643

phone number: +33 (0) 2 23 23 56 55

The authors have no conflict of interest in this work.

Abstract

$K_{0.5}Na_{0.5}NbO_3$ thin films were deposited by pulsed laser deposition on (100)MgO substrates for microwave device applications. A fine epitaxial growth of pure perovskite phase was evidenced by X-ray diffraction. Dielectric characterizations were performed from 1 to 40 GHz using coplanar microwave devices printed on the 500 nm-thick $K_{0.5}Na_{0.5}NbO_3$ thin films. Dielectric permittivity ε_r = 355 and loss tangent $tan\delta$ = 0.35 at 10 GHz were retrieved without biasing. A comparison of the results with those retrieved from the resonant cavity

method (to characterize as-deposited films) showed no deleterious influence neither from the device patterning nor the thin film-device interface. A frequency tunability up to 22% was measured under a moderate external DC bias electric field E_{bias} = 94 kV/cm. Temperature measurements from 20 to 240°C exhibited a permittivity increase up to ε_r = 975 coupled to a loss decrease $tan\delta$ = 0.25 at 10 GHz. According to such measurements, an orthorhombic-tetragonal phase transition was evidenced close to 220°C with an increase of the frequency tunability up to 34%. Comparison of the properties of such films with those grown on R-plane sapphire substrates demonstrated the benefit brought by the epitaxial growth of $K_{0.5}Na_{0.5}NbO_3$ films on (100) MgO.

Keywords: KNN, ferroelectric; thin film; tunable device; microwave

Introduction

Among the multifunctional oxides, ferroelectric materials are strongly investigated to push further the boundaries of the current technology. In that way, ferroelectric materials, also exhibiting piezoelectric behavior, are of great interest in many applications such as sensors, micro-electro-mechanical systems (MEMS) [1] or memory devices [2]. Their high dielectric permittivity ε_r values, that can be controlled by an external static electric field, present also a significant asset for miniature and tunable microwave device applications [3].

Due to its valuable properties, the ferroelectric $PbZr_{1-x}Ti_xO_3$ (PZT) oxide is currently considered as the most relevant ferroelectric material for many applications [4]. However, its well-known toxicity leads to an important effort of the scientific community to investigate lead-free alternative solutions. Among them, the perovskite $K_xNa_{1-x}NbO_3$ oxide (KNN) is studied as a promising candidate since Saito *et al.* reported a high piezoelectric coefficient d_{33} up to 300 pC/N [5]. Moreover KNN oxide exhibits a high Curie temperature ($T_c \approx$ 400°C)

depending upon its composition [6–8], valuable to expect the thermal stability of the KNN-based devices operating at room temperature. KNN is also known for (i) exhibiting at least one morphotropic phase boundary at room temperature in the neighborhood of the $K_{0.48}Na_{0.52}NbO_3$ composition [6, 9], and (ii) a polymorphic phase transition (PPT) between the room temperature orthorhombic phase and a higher temperature tetragonal one, also named $T_{O\text{-}T}$ [10, 11]. This last diffuse transition is usually expected between 180°C and 220°C [12, 13], where an increase of the dielectric characteristics was reported for the KNN and KNN-based ceramics at low frequency [14, 15]. In 2016, at microwave frequency and for bulk ceramic, Gao *et al.* reported an increase of the dielectric permittivity close to 220°C [16]. To improve the KNN overall properties, some groups focused on modifying the composition to shift such transition closer to room temperature. In 2014 for example, Wang *et al.* lowered both the Curie temperature down to 227°C and the polymorphic phase transition, and raised the low temperature rhombohedral-orthorhombic transition to build a new rhombohedral-tetragonal phase boundary close to room temperature. As a result, they obtained a piezoelectric coefficient d_{33} equal to ~ 490 pC/N [17].

Microwave dielectric characteristics of KNN thin films have been reported only in a few studies [16, 18–21]. For the $K_{0.5}Na_{0.5}NbO_3$ composition, Peddigari *et al*. measured a dielectric permittivity ε_r = 287 and loss tangent $tan\delta$ = 0.01 at 10 GHz [20]. At 20 GHz, Kim *et al.* reported the value $tan\delta$ = 0.23 (ε_r value not available) with a capacitance tunability of 22 % under an external biasing electric field E_{bias} = 200 kV/cm [21]. In our previous study, the dielectric characteristics (ε_r = 360 ; $tan\delta$ = 0.35) at 10 GHz were reported with a frequency tunability of 15% under a lower external biasing electric field E_{bias} = 80 kV/cm [22]. Thin films prepared by Peddigari *et al.* were deposited on Pt/Si and quartz substrates, those of Kim *et al.* on Nd:$YAlO_3$ substrates, and ours on R-cut sapphire substrates, which can explain the

difference of the reported values, as structural characteristics are known to influence the material ferroelectric properties [22]. Up to now, no direct study has focused on the substrate and temperature influences on the dielectric properties and characteristics of such films at microwaves. It is within this framework that the present study is involved.

Structural properties of $K_{0.5}Na_{0.5}NbO_3$ thin films deposited on (100)MgO substrates and their influence on the microwave responses of the tunable based-devices were investigated and compared with those of $K_{0.5}Na_{0.5}NbO_3$ films grown on R-cut sapphire substrates. Both substrates, useful for microwave applications ($\varepsilon_r \approx 10$ and $tan\delta \approx 10^{-4}$ at room temperature and 10 GHz), lead to various thin film structural qualities. On the one hand, R-cut sapphire is widely used for microwave electronic devices due to its relevant dielectric characteristics and its high robustness and chemical stability. On the other hand, MgO substrate is mechanically less resistant and more sensitive to moisture. However, the lattice constant of the cubic MgO substrate (a = 4.2 Å, JCPDS file #00-045-0946) is closer to those of the pseudo-cubic KNN (i.e. $a_{pc} \approx 4$ Å, $\beta \approx 90°$) [23, 24], unlike those of the sapphire substrate (rhombohedral, a = 4,758 Å and c = 12,991 Å in the hexagonal setting). Temperature-dependent dielectric behaviors of such films deposited on both substrates were also investigated up to 240°C.

Experimental section

2.1. Elaboration of KNN thin films by pulsed laser deposition (PLD)

$K_{0.5}Na_{0.5}NbO_3$ powder was first synthesized at 940°C for 4 hours in air by solid state reaction from sodium carbonate Na_2CO_3 (RP NORMAPUR 99.8%), anhydrous potassium carbonate K_2CO_3 (ACROS Organics 99%) and niobium oxide Nb_2O_5 (Alfa Aesar 99.5%) powders in stoichiometric quantity. A 60%$_{mol}$ excess of potassium nitrate KNO_3 powder was added to the KNN powder to counterbalance the loss of potassium during the laser deposition due to its volatility. The powder was then uniaxially pressed into a 25 mm-diameter targets

and annealed up to 500°C in air for 3 hours. The final composition of the target analyzed by energy dispersive X-ray spectroscopy (EDXS) was K : Na : Nb = 0.9 : 0.5 : 1.

Thin films were deposited by pulsed laser deposition (PLD) from the target on 10 mm × 10 mm × 0.5 mm (100) MgO single crystal substrates. Before each deposition step, the substrates were cleaned in acetone and isopropanol ultrasonic baths for 5 min each. A KrF excimer laser (Coherent company, pulse duration 20 ns, λ = 248 nm) was used to ablate the KNN ceramic target. An energy of 210 mJ, a fluence of 2-3 J.cm^{-2}, a working frequency of 4 Hz, a target-substrate distance of 55 mm and a deposition temperature of 650°C under 0.3 mbar oxygen pressure were used. These parameters led to a deposition rate of ~12 nm/min. Film thickness of ~500 nm was used to fabricate the microwave devices. The same deposition parameters were replicated for the $K_{0.5}Na_{0.5}NbO_3$ growth on R-cut sapphire substrates to ensure a fair comparison of the thin films.

2.2. KNN thin film characterizations

Structural characteristics were investigated by X-ray diffraction (XRD) by using the θ–2θ mode of Bragg-Brentano diffractometer (D8 Advance, Bruker) equipped with a monochromatized *Cu* $K_{\alpha 1}$ wavelength (λ = 1.54056 Å), and ω-scan and φ-scan modes of a 4-circles diffractometer (D8 Discover, Bruker, *Cu* $K_{\alpha 1,2}$). The surface morphology and composition were investigated at 10 kV by scanning electron microscopy (SEM, *JSM 7100F, JEOL*) coupled with an energy dispersive X-ray spectroscopy detector (EDXS, *SDD X-Max 50mm^2, Oxford Instruments*). As the potassium element detection was highly sensitive to charge accumulation effect, a 5 nm–thick carbon layer was deposited before SEM observation to ensure optimal element detection. Film thicknesses were measured by SEM on transverse sections obtained from a fracture along a sample edge.

Secondary ion mass spectrometry (SIMS) was used to investigate the presence of Mg in the sample thickness thanks to a CAMECA IMS7f equipment. To avoid charge effect on the isolated surface a thin Au layer was deposited prior analysis.

2.3. KNN microwave characterizations

Dielectric characteristics and frequency tunability of the KNN thin films were investigated using coplanar waveguide (CPW) devices, as represented in Figure 1. The devices consist of three 50-Ω transmission lines (8 mm, 5 mm and 3 mm long) to retrieve the KNN dielectric characteristics (ε_r; $tan\delta$) and a CPW quarter-wavelength open-ended stub resonator designed to exhibit a resonance frequency F_r at *X*-band. Further details are reported elsewhere [25].

The devices were fabricated from a 2 µm-thick silver overlayer deposited on a 5 nm-thick titanium underlayer used here only to ensure the strong adhesion of the silver metallization onto the ferroelectric oxide film. The silver thickness was set at three times the skin depth value at 10 GHz (δ = 0.64 µm). The metal layers were deposited by RF magnetron sputtering at room temperature. Standard photolithography and wet etching processes were used to pattern the devices. To enforce the equipotential condition on both CPW grounds and to prevent any excitation of parasitic slotline mode, gold wire bondings (15 µm-diameter and 250 µm-length) were implemented.

Microwave measurements at room temperature were carried out from 1 to 40 GHz through a probe station coupled to a vector network analyzer (*VectorSTAR MS4644B, ANRITSU*) and a hot chuck system (S-1060, SIGMATONE) for temperature measurements from room temperature to 240°C. A maximum static electric field E_{bias} of 94 kV/cm was set at the stub resonator and 27 kV/cm at the transmission lines, resulting of the 150 V highest external *DC* bias voltage applied. Due to the inherent over etching of the wet etching process

used, the measured gap dimensions ($g_r \approx 16$ µm and $g_l \approx 53$ µm) are slightly larger than the expected ones (Figure 1).

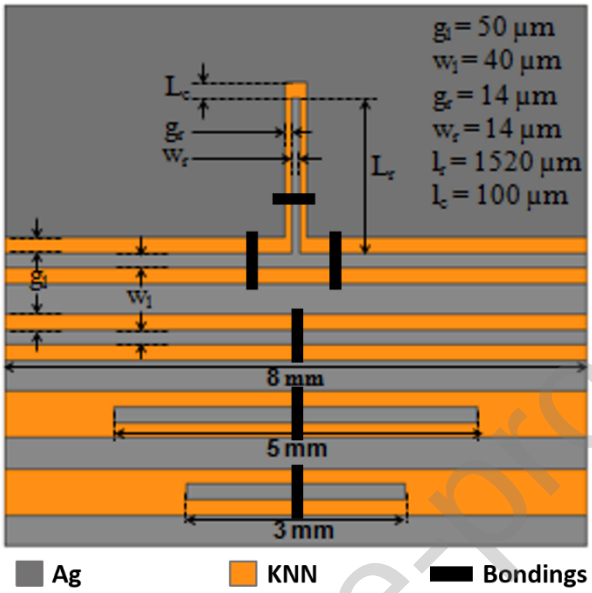

Figure 1. Layout and dimensions of the CPW devices

In this work, the structural and dielectric properties of the KNN thin films grown on MgO substrates are compared with previously reported properties of the KNN thin films grown on sapphire substrates [22]. Therefore, characterization methods were kept similar to ensure a relevant comparison.

Results and discussion

3.1. Composition, microstructure and structural properties of the KNN thin films

EDXS analyses correspond to the expected composition of the KNN thin films grown on (100) MgO substrates, namely $(K_{0.51}Na_{0.49})_{1.01}NbO_3$, corresponding therefore to the monoclinic phase. However, EDXS sensitivity is not suitable to detect accurately elements barely present in such films. Therefore, complementary SIMS analysis was performed to detect elements along the sample depth profile. This analysis highlights the presence of Mg

element into the films as shown in Figure 2. It may originate from a diffusion mechanism from the substrate into the KNN material during the deposition step. Such a diffusion along the film depth could appear surprising, but was already evidenced in $KTa_{0.65}Nb_{0.35}O_3$ thin films grown by PLD [26] and reported in other studies (such as in $Y_1Ba_2Cu_3O_{7-x}$ films deposited by sputtering [27]).

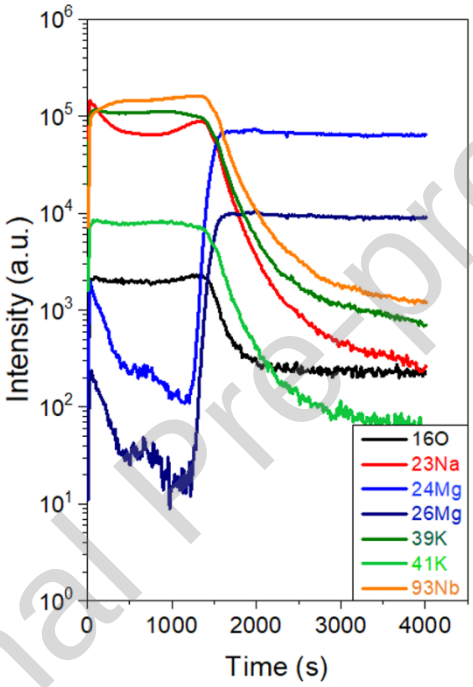

Figure 2. SIMS elemental depth profile of KNN/MgO

Morphology of the KNN thin films grown on MgO for the device fabrication is displayed in Figure 3. 500 nm-film thickness was measured from SEM cross section observation (inset in Figure 3). A crystalline orientation is observed through the homogeneous shape of the KNN grains and the high in-plane alignment. In a previous work on KNN thin films deposited on sapphire substrates, a similar grain shape was observed with a lower in-plane order [22].

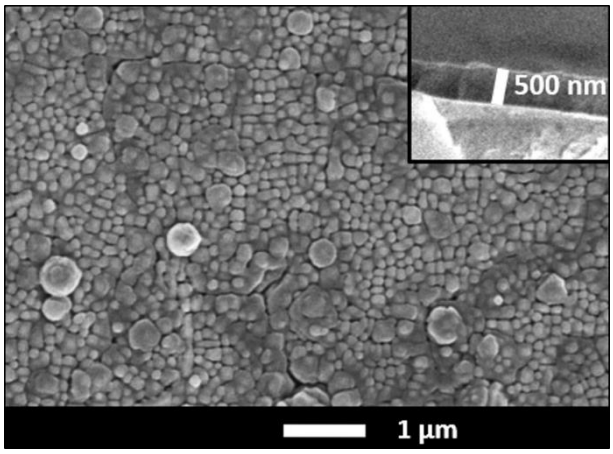

Figure 3. SEM image of the surface morphology and cross-section (in inset) of a KNN/MgO film

XRD patterns of KNN/MgO thin films are displayed in Figure 4. The θ-2θ pattern (Figure 4a) displays only reflections of the perovskite KNN phase, indexed with the monoclinic setting (for $K_{0.52}Na_{0.48}NbO_3$, a_m = 4.006 Å, b_m = 3.945 Å, c_m = 4.003 Å, β = 90.33°, JCPDS file #00-061-0316 [23, 24]). Note that the phase corresponding to the composition is usually described with orthorhombic or monoclinic unit cells. The relationship between those cell units is reported in Tellier *et al.* work [23]. The orthorhombic description is often considered as a more accurate description for this composition at room temperature. Nevertheless, the use of the monoclinic description enables a simpler comparison especially due to the direct relation with the cubic and pseudo-cubic description. In this work, the monoclinic description is used to match with the different studies on KNN thin films mentioned here. A preferential (100) orientation is evidenced by the strong peak at $2\theta \approx 22.2°$ together with a second (110) orientation corresponding to the weaker peak at $2\theta \approx 31.7°$.

XRD pattern does not show any (010) orientation, which was systematically observed on KNN thin films grown on sapphire substrates with the same deposition parameters [22]. However, the relative intensities of the 100 and 110 KNN peaks are similar on both substrates. The orientation factor of the 100 peak, computed by the Lotgering method [28], is

equal to 0.97. The lattice constants were determined as being $a_m \approx c_m \approx 4.00$ Å and $b_m \approx 3.95$ Å, similarly to those of the KNN/sapphire films [22]. Therefore, the presence of a small amount of Mg element in the thin film composition does not affect directly its structural properties, *i.e.* the lattice parameters remain in full agreement with those reported by Tellier *et al*. and Hondoko *et al*. for pure $K_{0.52}Na_{0.48}NbO_3$ perovskite material [23, 24].

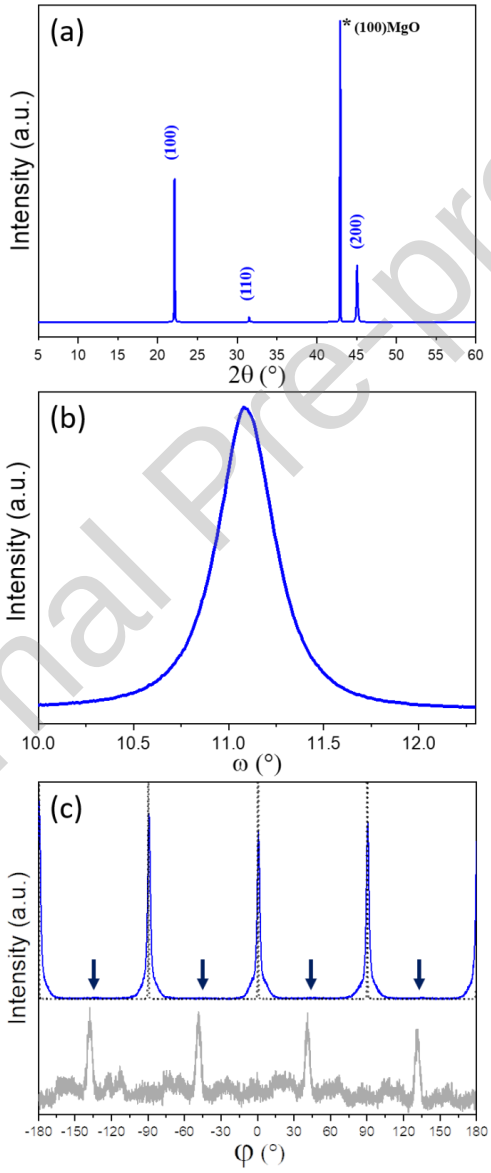

Figure 4. X-ray diffraction patterns of KNN/MgO thin film: (a) θ-2θ mode, (b) ω-scan on the 100 reflection and (c) φ-scan on the {110} planes of KNN/MgO (blue) and KNN/sapphire (gray) [22] (dashed-lines show the φ-scan pattern measured on the {220} MgO planes)

The sample crystalline quality was further investigated by ω-scans on the 100 reflection (Figure 4b) and φ-scan on the {110} planes (Figure 4c). The full-width-at-half-maximum (FWHM) $\Delta\omega = 0.35°$ indicates a well-textured thin film. The φ-scan exhibits four distinctive peaks at 90° apart from each other, aligned on the four peaks of the {220} MgO planes of the single crystal substrate. The narrow peaks and their relative positions evidence a high in-plane ordering quality of the KNN thin films with a "cube-on-cube" growth on the MgO substrate (~5% mismatch between the pseudo-cubic KNN lattice parameters and the cubic MgO ones). A second very minor in-plane orientation of the KNN crystallites at 45° is observed through four small rises from the background line at 45° of the substrate peaks (see the arrows in Figure 4c). It is worth noting that KNN thin films grown on R-plane sapphire substrates exhibited a similar quality of texturation ($\Delta\omega \approx 0.36°$ computed from the 100 ω-scan reflection) and showed some evidence of an epitaxial-like growth despite the large ~14% mismatch with the sapphire substrate. Nevertheless the intensity of the KNN φ-scan diffraction peaks remained very low on sapphire substrate, supporting mainly a texture-type crystalline quality (Figure 4c) [22]. The XRD analysis of the present study demonstrates an improvement of the KNN epitaxial quality promoted by the (100)MgO substrate (in agreement with the microstructure observed by SEM (Figure 3)).

3.2. KNN dielectric characteristics

3.2.1 Room temperature dielectric characteristics

The dielectric characteristics (ε_r; $tan\delta$) at room temperature of the KNN/MgO thin films were retrieved from the measured reflection (S_{11}) and transmission (S_{21}) coefficients on the CPW transmission lines (Figure 5a) [25, 29]. A permittivity $\varepsilon_r = 355$ and loss tangent $tan\delta = 0.35$ are obtained at 10 GHz. The fast decrease of the dielectric permittivity from 1 to 5 GHz

with and without biasing is attributed to the freezing of the polar domain motion, and that of *tanδ* to restriction in metal skin depth loss [25]. The permittivity value remains very close to that of the KNN thin films grown on sapphire substrates (ε_r = 360 at 10 GHz) [22], value retrieved from identical CPW devices in order to perform an accurate comparison. The present value ε_r = 355 is also higher than those previously reported on pure $K_{0.5}Na_{0.5}NbO_3$ thin films (ε_r = 287 at 10 GHz [20]) and even Dy_2O_3-doped KNN thin films (ε_r = 307 at 10 GHz [30]) grown on quartz substrates. The higher permittivity measured on both KNN/MgO and KNN/R-cut sapphire is attributed to the crystalline orientation and weak mosaicity of our samples, compared with the KNN polycrystalline growth reported by Peddigari *et al.* [20]. As permittivity, loss is also similar on both substrates [22]. Consequently, the resulting epitaxial growth of the KNN thin film on (100)MgO does not impact the (ε_r; *tanδ*) dielectric characteristics.

Focusing now on the KNN intrinsic loss, *tanδ* values are higher than those reported by Peddigari *et al.* (*tanδ* = 0.01 at 10 GHz [20]) and by Kim *et al.* (*tanδ* = 0.23 at 20 GHz [21]), although the absolute variation versus operating frequency remains small (*tanδ* = 0.35 at 5 GHz towards *tanδ* = 0.40 at 40 GHz). The different measurement methods used, *i.e* based or not on printed devices, can explain the divergence in the reported intrinsic loss values [31]. As such, comparison of the retrieved *tanδ* values from the transmission line measurements is relevant to investigate the impact of the Ag/Ti layers printed on the KNN films and the possible interface role between the metal layers and the ferroelectric oxide material. In that way, an analogous KNN/MgO sample has been elaborated and characterized by both methods, namely the present transmission line method and the resonant cavity method, which does not require any printed devices. Details on this specific method are reported elsewhere

[31]. The dielectric characteristics measured at 12.3 GHz from both methods are summarized in Table 1. No major difference is observed. The variation of ε_r from 330 to 300 and of *tanδ* from 0.38 to 0.35 is attributed to a possible inhomogeneity of the KNN layer thickness over the entire samples area (estimated to be close to 10%). Indeed, the thickness error remains the major source of uncertainty in such characterizations. Therefore, in this study, the printed device itself and the related measurement technique have no impact on the retrieved KNN intrinsic loss. Another hypothesis to explain the difference between the *tanδ* values measured here and those reported in [20, 30] can be the density difference between the KNN layers grown by PLD technique and those by magnetron sputtering technique. Further investigations are required to reinforce the present assumption.

Table 1 Dielectric permittivity ε_r and loss tangent *tanδ* of KNN/MgO at 12.3 GHz retrieved from the resonant cavity and transmission line methods

	Resonant cavity method		**Transmission line method**	
Sample	$\boldsymbol{\varepsilon_r}$	***tanδ***	$\boldsymbol{\varepsilon_r}$	***tanδ***
KNN/MgO	300	0.35	330	0.38

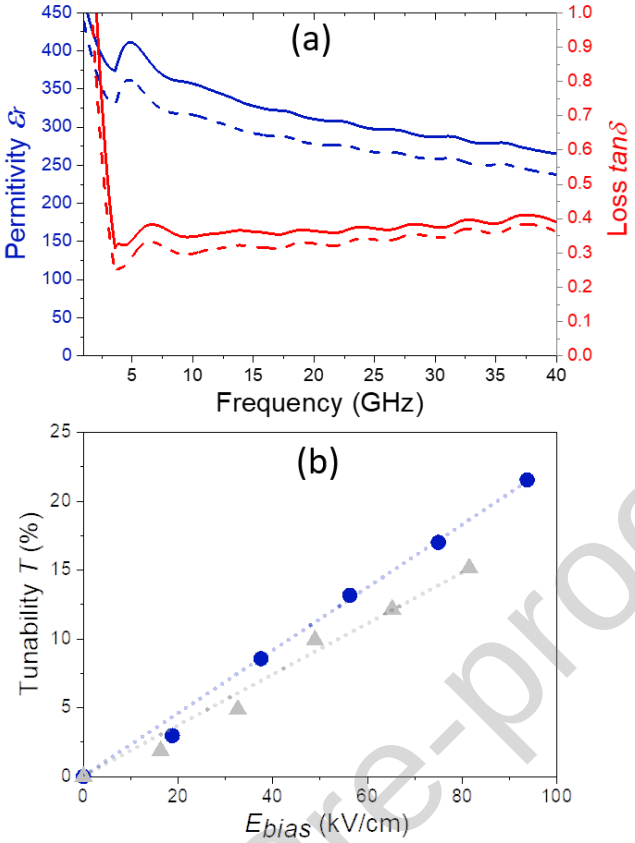

Figure 5. (a) Frequency dependence of the dielectric permittivity ε_r (blue) and loss tangent *tanδ* (red) of KNN/MgO measured at room temperature without (solid line) and under (dashed line) biasing E_{bias} = 27 kV/cm; (b) measured frequency tunability T under various E_{bias} of the KNN/MgO (blue dot) and the KNN/sapphire (gray triangle) samples [22]

The frequency tunability T was computed from the variation of the resonance frequency F_r (frequency value at the minimum S_{21} parameter) of the CPW stub resonator printed on the KNN film under various E_{bias} values, as follows:

$$T(\%) = \frac{|F_r(E_{bias}=0) - F_r(E_{bias})|}{F_r(E_{bias}=0)} \times 100 \quad (1)$$

The 150 V highest applied voltage leads to a maximum external *DC* electric field $E_{bias} \approx 90$ kV/cm. A frequency tunability equal to 22% is obtained from F_r = 10.5 GHz (without biasing) up to F_r = 12.8 GHz (under E_{bias} = 94 kV/cm). The tunability of the KNN films grown on MgO substrates is therefore higher than that measured on KNN/sapphire (T = 17% and T =

15% under E_{bias} = 80 kV/cm, respectively). This result was checked on several batches of samples. Moreover, a frequency tunability of 20 % and higher has been repeatedly measured on the KNN/MgO samples. Accordingly, the increase of the frequency tunability is attributed to the better KNN epitaxial growth on MgO substrates. This result is consistent with the general inclination of epitaxial thin films to exhibit a more single-crystal-like behavior, as single crystal often exhibits improved dielectric properties compared with those of their bulk counterpart.

3.2.2 Temperature-dependent dielectric characteristics

To further characterize the KNN thin film properties, dielectric measurements were performed as a function of temperature. Figure 6 (a) and Figure 6 (b) present the dielectric characteristics (ε_r; $tan\delta$ respectively) variation of the KNN thin films retrieved from the measured reflection (S_{11}) and transmission (S_{21}) coefficients of the CPW transmission lines at 10 GHz from 20°C to 240°C working temperature. Note that Figure 6 (c) presents the variation of the resonance frequency F_r of the CPW sub resonator printed on KNN/MgO from 20°C to 220°C. To investigate the influence of the substrate, the dielectric characteristics of the KNN/MgO sample are compared with those of the previously mentioned KNN/sapphire sample.

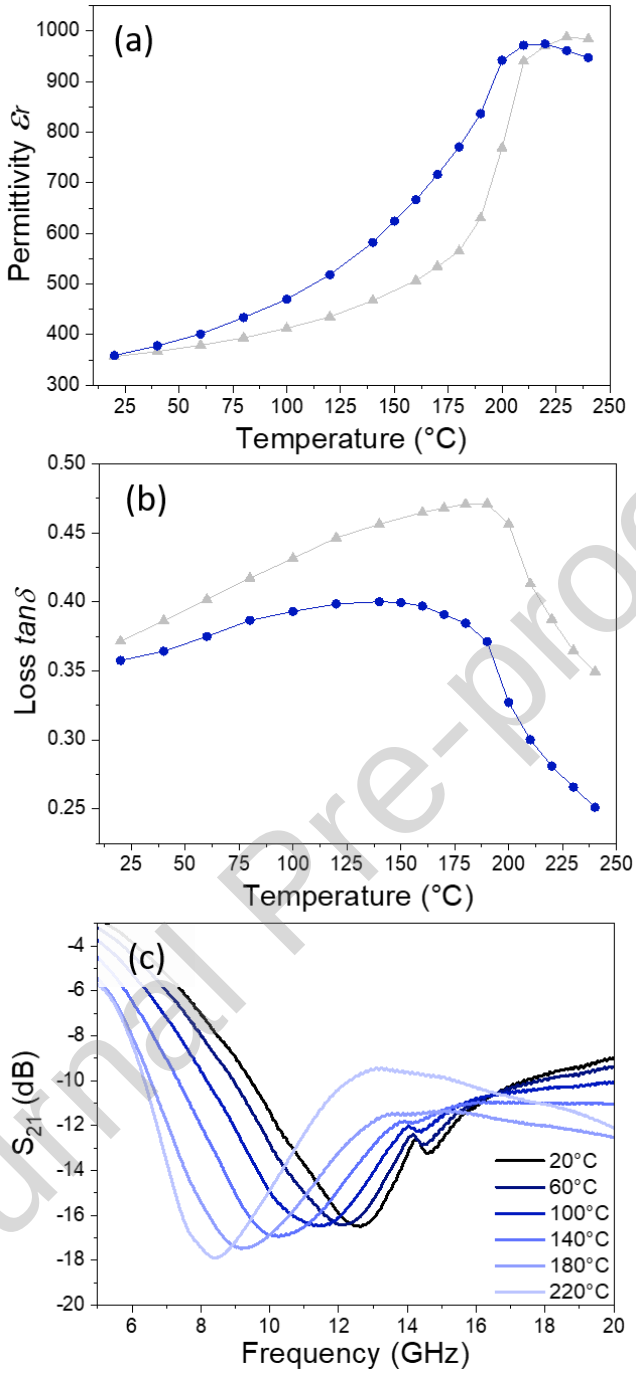

Figure 6. Temperature-dependent dielectric characteristics: (a) permittivity ε_r ; (b) loss tangent $tan\delta$ of 500 nm-thick KNN/MgO sample (blue dot) and 510 nm-thick KNN/sapphire sample (gray triangle) at 10 GHz. (c) Transmission coefficient S_{21} variation vs. temperature of the stub resonator printed on the KNN/MgO sample

Both samples exhibit a permittivity increase versus the temperature, as expected for ferroelectric materials when the temperature is racing towards the Curie temperature (close to 400-420°C here). The increase of the permittivity leads directly to the decrease of the stub resonance frequency, from 12.6 GHz at 20°C to 8.2 GHz at 220°C (Figure 6(c)). A maximum of permittivity (ε_r = 975) is reached at 210°C-220°C for the KNN/MgO sample where a similar one (ε_r = 990) is reached at 230°C for the KNN/sapphire sample. This maximum of permittivity is typical of the diffuse PPT, usually reported between 180°C and 220°C [12, 13]. Similar permittivity behaviors have been reported in literature on ceramics and at low frequency with a first ε_r maximum at the $T_{O\text{-}T}$ transition before reaching the maximum at the Curie temperature [13, 15, 32, 33]. On ceramic and at microwave frequencies, Gao *et al.* reported a large permittivity increase [16]. A first and weak increase begins from 100 up to 210°C followed by a sharp increase at 220°C. In the present study, KNN/sapphire sample exhibits a first and gentle slope from 20°C to 180°C, followed by the sharp increase up to 230°C. Regarding the KNN/MgO sample, the permittivity increases in a more continuous way. This difference in temperature behavior is ascribed to an epitaxial growth effect that is the major difference between the KNN/MgO and KNN/sapphire samples. Complementary investigations are currently ongoing to detail the phenomenon occurring.

Even though transition temperature characteristics are influenced by strains [34] and routinely associated with epitaxial growth, it is not the case here due to the quite great thickness of the KNN/MgO film (500 nm) promoting strain relaxation. Moreover and as previously presented, SIMS analyses evidenced the presence of Mg element into the KNN film. The resulting Mg-doped film can explain the observed slight shift in transition temperature. Such Mg-doping effect in transition temperature was also reported in other systems, such as Ba-Zr-Ti-O system [35]. Furthermore, in ceramic KNN materials, Malic *et*

al. evidenced by differential scanning calorimetry a T_{O-T} shift temperature towards a lower temperature after doping of the ceramic with $0.5\%_{mol}$ of Mg [36].

Similarly to the permittivity temperature variation, a slight monotonous *tanδ* variation is observed from *tanδ* = 0.35 to *tanδ* = 0.40 on KNN/MgO sample compared with that on KNN/sapphire sample from 0.37 to 0.47. As *tanδ* value is defined as the ratio of the imaginary part of the complex dielectric permittivity on its real part, and as its imaginary part depends on the material electric conductivity [37], such increase is therefore consistent. Afterwards, the decrease of *tanδ* exhibited by the KNN/MgO sample begins at 140°C followed by a sharp decrease at 180°C to achieve *tanδ* = 0.25 at 240°C. For the KNN/sapphire sample, the sharp decrease begins directly at 190°C, thereby confirming the 10-20°C transition temperature shift, to achieve *tanδ* = 0.34 at 240°C. A similar decrease of *tanδ* value near the T_{O-T} transition has also been reported at lower frequency (100 kHz) by Mgbemere *et al.* [15] and Pavlic *et al.* [33].

Although a significant decrease of the KNN loss was achieved, new attempts are expected to further restrict it in view of microwave device applications. Some solutions are readily available, such as ferroelectric/dielectric multilayers deposition [38] or by confining the ferroelectric layer into the efficient regions of the microwave devices [39].

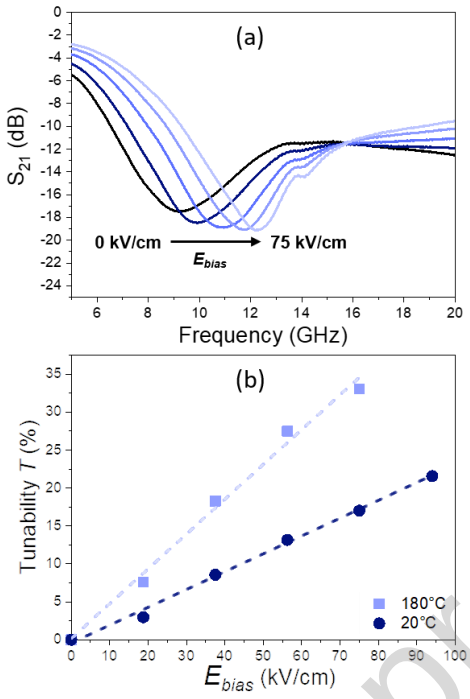

Figure 7. (a) Transmission coefficient S_{21} variation and (b) frequency tunability T, both measured at 180°C on the stub resonator printed on the KNN/MgO sample under various external electric field E_{bias} (dashed lines are guide for the eye)

Frequency tunability measurements were also performed on the stub resonator printed on the KNN/MgO sample at 180°C (Figure 7). The resonance frequency varies from 9.1 GHz (no biasing) to 12.2 GHz (E_{bias} = 75 kV/cm). Temperature increase leads to a twofold increase of the tunability (T = 34%) at 180°C under a relative low biasing electric field (E_{bias} = 75 kV/cm) compared with that at room temperature under the same E_{bias} value (T = 17%).

4. Conclusion

The dielectric characteristics (ε_r; $tan\delta$) and the frequency tunability T of $K_{0.5}Na_{0.5}NbO_3$ thin films epitaxially grown on (100)MgO substrates were studied at microwaves. At room temperature, a frequency tunability T = 22% under E_{bias} = 94 kV/cm was measured on stub resonators printed on such films. The increase of tunability compared with that measured on

KNN/R-plane sapphire sample (T = 15%) is assigned to the KNN epitaxial-like growth on MgO substrates.

Variation of the dielectric characteristics versus temperature at microwaves was also investigated from 20 to 240°C. The temperature-dependent dielectric characterization shows a diffuse orthorhombic-tetragonal polymorphic phase transition which is also slightly influenced by the type of the substrate. At the O-T transition temperature, a dielectric permittivity value ε_r higher than 950 is reached at 10 GHz with a lower loss tangent value ($tan\delta$ = 0.25), promoting the potentialities of the KNN lead-free ferroelectric material for tunable devices at microwaves. In order to shift such properties at room temperature, the O-T transition should be lowered. Doping or substitution in thin film composition may be studied through complementary investigations.

Acknowledgments

The authors are grateful for the financial support of the Direction Générale de l'Armement (DGA) and the Région Bretagne (PhD research Grant of B.A, project ARMin). This work was also supported by the European Union through the European Regional Development Fund (ERDF), the Ministry of Higher Education and Research, the Région Bretagne, the Département des Côtes d'Armor and Saint-Brieuc Armor Agglomération, through the CPER Projects 2015-2020 MATECOM and SOPHIE / STIC & Ondes. ScanMAT, UMS 2001 CNRS-University of Rennes 1, received a financial support from the Région Bretagne, the Département d'Ille et Vilaine and the European Union (2015-2020 CPER projects SCANMAT and Verres). S. Ollivier is warmly acknowledged for her assistance in thin film deposition and characterization. C. Derouet is warmly acknowledged for his technical assistance in X-Ray diffraction. Francis Gouttefangeas and Loic Joanny are

also warmly acknowledged for SEM observations and EDXS analyses (ScanMAT - CMEBA facilities).

References

[1] Polla DL (1995) Microelectromechanical systems based on ferroelectric thin films. *Microelectron. Eng.* 29:51–58. doi: 10.1016/0167-9317(95)00114-X

[2] Östling M, Koo S-M, Zetterling C-M, Khartsev S, and Grishin A (2004) Ferroelectric thin films on silicon carbide for next-generation nonvolatile memory and sensor devices. *Thin Solid Films* 469–470:444–449. doi: 10.1016/j.tsf.2004.09.030

[3] Petosa A (2012) An overview of tuning techniques for frequency-agile antennas. *IEEE Antennas Propag. Mag.* 54:271–296. doi: 10.1109/MAP.2012.6348178

[4] Ishchuk V, Kuzenko D, and Sobolev V (2018) Piezoelectric and functional properties of materials with coexisting ferroelectric and antiferroelectric phases. *AIMS Mater. Sci.* 5:711–741, 2018, doi: 10.3934/matersci.2018.4.711

[5] Saito Y, Takao H, Tani T, Nonoyama T, Takatori K, Homma T, Nagaya T, and Nakamura M (2004) Lead-free piezoceramics. *Nature* 432:84–87. doi: 10.1038/nature03028

[6] Ahtee M, and Glazer AM (1976) Lattice parameters and tilted octahedra in sodium–potassium niobate solid solutions. *Acta Crystallogr. Sect. A* 32:434–446. doi: 10.1107/S0567739476000983

[7] Tennery VJ, and Hang KW (1968) Thermal and X-ray diffraction studies of the $NaNbO_3$–$KNbO_3$ system. *J. Appl. Phys.* 39:4749–4753. doi: 10.1063/1.1655833

[8] Shirane G, Newnham R, and Pepinsky R (1954) Dielectric properties and phase transitions of $NaNbO_3$ and $(Na,K)NbO_3$. *Phys. Rev.* 96:581–588. doi: 10.1103/PhysRev.96.581

[9] Wu L, Zhang JL, Wang CL, and Li JC (2008) Influence of compositional ratio K/Na on physical properties in $(K_xNa_{1-x})NbO_3$ ceramics. *J. Appl. Phys.* 103:084116. doi: 10.1063/1.2907866

[10] Li J-F, Wang K, Zhu F-Y, Cheng L-Q, and Yao F-Z (2013) $(K,Na)NbO_3$-based lead-free piezoceramics: Fundamental aspects, processing technologies, and remaining challenges. *J. Am. Ceram. Soc.* 96:3677–3696. doi: 10.1111/jace.12715

[11] Dai Y, Zhang X, and Zhou G (2007) Phase transitional behavior in $K_{0.5}Na_{0.5}NbO_3$–$LiTaO_3$ ceramics. *Appl. Phys. Lett.* 90:262903. doi: 10.1063/1.2751607

[12] Hewat AW (1973) Cubic-tetragonal-orthorhombic-rhombohedral ferroelectric transitions in perovskite potassium niobate: neutron powder profile refinement of the structures. *J. Phys. C Solid State Phys.* 6:2559–2572. doi: 10.1088/0022-3719/6/16/010

[13] Singh K, Lingwal V, Bhatt SC, Panwar NS, and Semwal BS (2001) Dielectric properties of potassium sodium niobate mixed system. *Mater. Res. Bull.* 36:2365–2374. doi: 10.1016/S0025-5408(01)00711-5

[14] Huan Y, Wei T, Wang Z, Lei C, Chen F, and Wang X (2019) Polarization switching and rotation in KNN-based lead-free piezoelectric ceramics near the polymorphic phase boundary. *J. Eur. Ceram. Soc.* 39:1002–1010. doi: 10.1016/j.jeurceramsoc.2018.11.001

[15] Mgbemere HE, Hinterstein M, and Schneider GA (2012) Structural phase transitions and electrical properties of $(K_xNa_{1-x})NbO_3$-based ceramics modified with Mn. *J. Eur. Ceram. Soc.* 32:4341–4352. doi: 10.1016/j.jeurceramsoc.2012.07.033

[16] Gao L, Zhou W, Luo F, and Zhu D (2017) Dielectric properties in the microwave range of $K_{0.5}Na_{0.5}NbO_3$ ceramics. *J. Electron. Mater.* 46:123–129. doi: 10.1007/s11664-016-4853-2

[17] Wang X, Wu J, Xiao D, Zhu J, Cheng X, Zheng T, Zhang B, Lou X, and Wang X (2014) Giant piezoelectricity in potassium–sodium niobate lead-free ceramics. *J. Am. Chem. Soc.* 136:2905–2910. doi: 10.1021/ja500076h

[18] Abadei S, Cho C-R, Grishin A, and Gevorgian S (2001) Low frequency characterisation of laser ablation deposited thin $Na_{0.5}K_{0.5}NbO_3$ (*NKN*) films for microwave application. *Ferroelectrics* 263:173–179. doi: 10.1080/00150190108225195

[19] Gao L, Zhou W, Luo F, Zhu D, and Yang Z (2016) Microwave dielectric properties of potassium sodium niobate ceramics with different K/Na ratios. *Ceram. Int.* 42:19105–19109. doi: 10.1016/j.ceramint.2016.09.071

[20] Peddigari M, Sindam B, Raju KCJ, and Dobbidi P (2015) Optical and microwave dielectric properties of phase pure $(K_{0.5}Na_{0.5})NbO_3$ thin films deposited by RF magnetron sputtering. *J. Am. Ceram. Soc.* 98:1444–1452. doi: 10.1111/jace.13502

[21] Kim J-Y and Grishin AM (2006) Niobate-tantalate thin films microwave varactors. *Thin Solid Films* 515:619–622. doi: 10.1016/j.tsf.2005.12.212

[22] Aspe B, Cissé F, Castel X, Demange V, Députier S, Ollivier S, Bouquet V, Joanny L, Sauleau R, and Guilloux-Viry M (2018) $K_xNa_{1-x}NbO_3$ perovskite thin films grown by pulsed laser deposition on R-plane sapphire for tunable microwave devices. *J. Mater. Sci.* 53:13042–13052. doi: 10.1007/s10853-018-2593-9

[23] Tellier J, Malic B, Dkhil B, Jenko D, Cilensek J, and Kosec M (2009) Crystal structure and phase transitions of sodium potassium niobate perovskites. *Solid State Sci.* 11:320–324. doi: 10.1016/j.solidstatesciences.2008.07.011

[24] Handoko AD, and Goh GKL (2010) Hydrothermal synthesis of sodium potassium niobate solid solutions at 200°C. *Green Chem.* 12:680. doi: 10.1039/b923840a

[25] Simon Q, Corredores Y, Castel X, Benzega R, Sauleau R, Mahdjoubi M, Le Febvrier A, Députier S, Guilloux-Viry M, Zhang LY, Laurent P, and Tanné G (2011) Highly tunable microwave stub resonator on ferroelectric $KTa_{0.5}Nb_{0.5}O_3$ thin film. *Appl. Phys. Lett.* 99:092904. doi: 10.1063/1.3626040

[26] Simon Q, Bouquet V, Demange V, Députier S, Wyczisk F, Garry G, Ziaie A, and Guilloux-Viry M (2011) Mg diffusion in $K(Ta_{0.65}Nb_{0.35})O_3$ thin films grown on MgO evidenced by Auger electron spectroscopy investigation. *Appl. Surf. Sci.* 257:9485–9489. doi: 10.1016/j.apsusc.2011.06.041

[27] Lemaître Y, Mansart D, Marcilhac B, Garcia-Lopez J, Siejka J, and Mage JC (1997) Evidence of a 'notch effect' in microwave surface resistance versus deposition temperature for $Y_1Ba_2Cu_3O_{7-x}$ thin film on MgO (100) substrate. *J. Alloys Compd.* 251:166–171. doi: 10.1016/S0925-8388(96)02793-4

[28] Lotgering FK (1959) Topotactical reactions with ferrimagnetic oxides having hexagonal crystal structures—I. *J. Inorg. Nucl. Chem.* 9:113–123. doi: 10.1016/0022-1902(59)80070-1

[29] Carlsson E, and Gevorgian S (1999) Conformal mapping of the field and charge distributions in multilayered substrate CPWs. *IEEE Trans. Microw. Theory Tech.* 47:1544–1552. doi: 10.1109/22.780407

[30] Peddigari M, Patel V, Bharti GP, Khare A, and Pamu D (2017) Microwave dielectric and nonlinear optical studies on radio-frequency sputtered Dy_2O_3-doped KNN thin films. *J. Am. Ceram. Soc.* 100:3013–3023. doi: 10.1111/jace.14846

[31] Queffelec P, Laur V, Chevalier A, Le Floch J-M, Passerieux D, Cros D, Madrangeas V, Le Febvrier A, Députier S, Guilloux-Viry M, Houzet G, Lacrevaz T, Bermond C, and Fléchet B (2014) Intercomparison of permittivity measurement techniques for ferroelectric thin layers. *J. Appl. Phys.* 115:024103. doi: 10.1063/1.4858388

[32] Liu Y, Du Y, Cheng C, Sun X, Jiang N, Wang J, and Sun X (2019) Dielectric and impedance spectroscopy analysis of lead-free $(1-x)(K_{0.44}Na_{0.52}Li_{0.04})(Nb_{0.86}Ta_{0.10}Sb_{0.04})O_3$-$xBaTiO_3$ ceramics. *Ceram. Int.* 45:13347–13353. doi: 10.1016/j.ceramint.2019.04.029

[33] Pavlič J, Malič B, and Rojac T (2014) Microstructural, structural, dielectric and piezoelectric properties of potassium sodium niobate thick films. *J. Eur. Ceram. Soc.* 34:285–295. doi: 10.1016/j.jeurceramsoc.2013.09.001

[34] Von Helden L, Bogula L, Janolin P-E, Hanke M, Breuer T, Schmidbauer M, Ganschow S, and Schwarzkopf J (2019) Huge impact of compressive strain on phase transition temperatures in epitaxial ferroelectric $K_xNa_{1-x}NbO_3$ thin films. *Appl. Phys. Lett.* 114:232905. doi: 10.1063/1.5094405

[35] Xu Y, Zhang K, Fu L, Tong T, Cao L, Zhang Q, and Chen L (2019) Effect of MgO addition on sintering temperature, crystal structure, dielectric and ferroelectric properties of lead-free BZT ceramics. *J. Mater. Sci. Mater. Electron.* 30:7582–7589. doi: 10.1007/s10854-019-01073-x

[36] Malic B, Bernard J, Holc J, Jenko D, and Kosec M (2005) Alkaline-earth doping in (K,Na)NbO_3 based piezoceramics. *J. Eur. Ceram. Soc.* 25:2707–2711. doi: 10.1016/j.jeurceramsoc.2005.03.127

[37] Cao M-S, Song W-L, Hou Z-L, Wen B, and Yuan J (2010) The effects of temperature and frequency on the dielectric properties, electromagnetic interference shielding and microwave-absorption of short carbon fiber/silica composites. *Carbon* 48:788–796. doi: 10.1016/j.carbon.2009.10.028

[38] Corredores Y, Le Febvrier A, Castel X, Sauleau R, Benzerga R, Députier S, Guilloux-Viry M, Mekadmini A, Martin N, and Tanné G (2014) Study of ferroelectric/dielectric multilayers for tunable stub resonator applications at microwaves. *Thin Solid Films* 553:109–113. doi: 10.1016/j.tsf.2013.11.068

[39] Corredores Y, Simon Q, Benzerga R, Castel X, Sauleau R, Le Febvrier A, Députier S, Guilloux-Viry M, Zhang LY, and Tanné G (2014) Loss Reduction Technique in Ferroelectric Tunable Devices by Laser Microetching. Application to a CPW Stub Resonator in X-Band. *IEEE Trans. Electron Devices* 61:4166–4170. doi: 10.1109/TED.2014.2360846

Graphical abstract

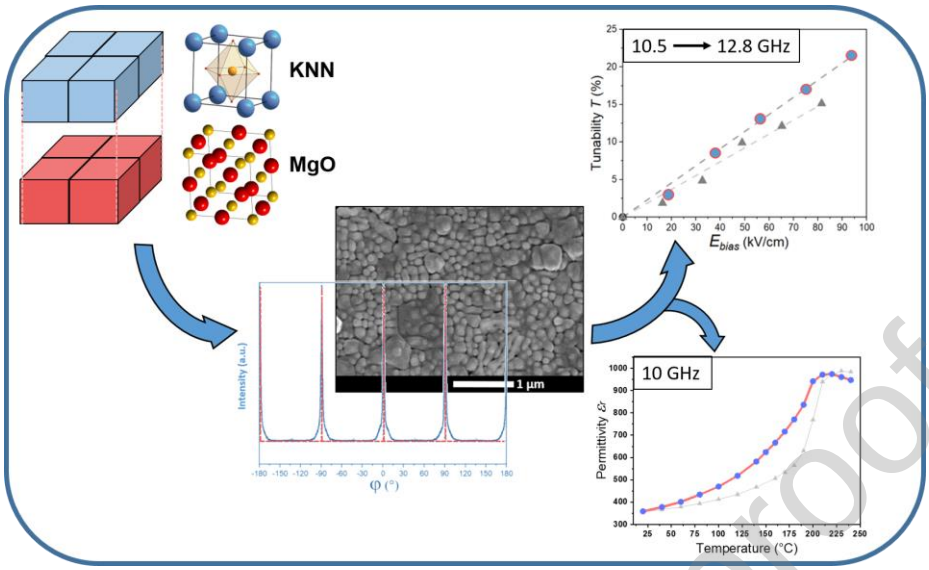

Credit Authors Statement

B. Aspe: Conceptualization, Formal Analysis, Investigation, Writing – Original draft, Visualization

X. Castel: Conceptualization, Formal Analysis, Investigation, Supervision, Writing – Original draft, Visualization, funding acquisition

V. Demange: Conceptualization, Formal Analysis, Investigation, Writing, Visualization

D. Passerieux: Conceptualization, Formal Analysis, Investigation

M.A. Pinault-Thaury: Conceptualization, Formal Analysis, Investigation, Visualization, Writing

F. Jomard: Conceptualization, Formal Analysis, Investigation, Visualization

S. Députier: Conceptualization, Investigation, Resources, Writing

D. Cros: Conceptualization, Formal Analysis, Investigation, Writing

V. Madrangeas: Conceptualization, Formal Analysis, Investigation, Writing

V. Bouquet: Conceptualization, Resources, Investigation, Writing

R. Sauleau: Conceptualization, Formal Analysis, Investigation, Supervision, Writing, Visualization, funding acquisition

M. Guilloux-Viry: Conceptualization, Investigation, Supervision, Writing, Original draft, Project Administration, funding acquisition

Declaration of interests

☒ The authors declare that they have no known competing financial interests or personal relationships that could have appeared to influence the work reported in this paper.

☐The authors declare the following financial interests/personal relationships which may be considered as potential competing interests:

Highlights:

- Epitaxial KNN perovskite thin films deposited by PLD on (100)MgO
- The structural characteristics of KNN thin films grown on (100)MgO benefit the frequency tunability of microwave devices, evidenced by the higher value of the tunability when compared to KNN thin films deposited on sapphire substrate
- The investigation of the dielectric characteristics (ε_r, tanδ) at 10 GHz between 20°C and 240°C that shows the polymorphic phase transition (PPT) of the KNN thin films
- The frequency tunability measured on a stub resonator at 180°C which emphasizes its enhancement in the vicinity of the PPT transition.